NASA-CR-193397

Photometry and Spectroscopy in the Open Cluster α Persei. II.

NAGW-2698

Charles F. Prosser

Harvard-Smithsonian Center for Astrophysics,
60 Garden St. MS-66,
Cambridge, MA 02138

GRANT
IN-89-CR
OCIT
185971
P- 31

Abstract

Results from a combination of new spectroscopic and photometric observations in the lower main-sequence and pre-main sequence of the open cluster α Persei are presented. New echelle spectroscopy has provided radial and rotational velocity information for thirteen candidate members, three of which are nonmembers based on radial velocity, absence of a Li 6707Å feature, and absence of Hα emission. A set of revised rotational velocity estimates for several slowly rotating candidates identified earlier is given, yielding rotational velocities as low as 7 km/s for two apparent cluster members. VRI photometry for several pre-main sequence members is given; the new (V,V$-$I$_K$) photometry yields a more clearly defined pre-main sequence. A list of $\sim$ 43 new faint candidate members based on the (V,V$-$I$_K$) CCD photometry is presented in an effort to identify additional cluster members at very low masses. Low-dispersion spectra obtained for several of these candidates provide in some cases supporting evidence for cluster membership. The single brown dwarf candidate in this cluster is for the first time placed in a color-magnitude diagram with other cluster members, providing a better means for establishing its true status. Stars from among the list of new photometric candidates may provide the means for establishing a sequence of cluster members down to very faint magnitudes (V$\sim$ 21) and consequently very low masses. New coordinate de--minations for previous candidate members and finding charts for the new photometric candidates are provided in appendices.

(NASA-CR-193397) PHOTOMETRY AND SPECTROSCOPY IN THE OPEN CLUSTER ALPHA PERSEI, 2 (Harvard-Smithsonian Center for Astrophysics) 31 p

N94-14358

Unclas

G3/89 0185971

1. Introduction

In the study of open clusters as a means of understanding pre-main sequence stellar evolution, the α Persei cluster has received increased attention in recent years. Continuing the work begun by Heckmann etal. (1956,1958), Mitchell (1960), and Petrie & Heard (1970), new membership studies have resulted in the identification of numerous low-mass, pre-main sequence members (Stauffer etal. 1985,1989; Prosser 1992; Trullols etal. 1989). A more nearly complete review of previous research on α Per is given in Prosser (1992). The faint cluster members recovered in these recent studies provide important information for the early evolution of low-mass stars and may be compared with the slightly older, low-mass members of the Pleiades.

In this paper we report on new, more accurate, photometry and new echelle spectra for previously known members reported in Prosser (1992, = Paper I). We also present revised $v \sin i$ estimates for slow rotators and a list of new candidate members selected photometrically, whose membership in α Per is supported in some cases by low-dispersion spectra obtained at Hα. Improved coordinates for the AP stars originally reported in Prosser (1992) are given in an appendix.

2. Echelle Spectra.

2.1 New Observations

It was seen in Paper I, and in fact recognized previously by others (e.g. Petrie & Heard 1970), that proper motion and photometric surveys alone in α Per would fail to eliminate all nonmembers. Radial velocity measures were needed to further identify nonmembers or confirm membership for candidate members. Echelle observations in Paper I provided not only radial velocities, but also rotational velocity ($v \sin i$) estimates, information on possible binaries, and indications of the presence of Li 6707 and/or Hα emission. As part of an overall program to study the lower main sequence of α Per and obtain the rotational velocity distribution and binary frequency, we have obtained additional high-dispersion spectra for several α Per candidate members given in Paper I.

As in Paper I, the new echelle spectra were obtained using the Hamilton echelle spectrograph (Vogt 1987) with the Lick 3m telescope. The data was obtained and reduced in the same manner as described in Paper I and we refer the reader there for the details. Errors in the determined radial velocity for a star depended on rotational velocity and varied from $\sim \pm 0.8$ km/s for slow rotators ($v \sin i \leq 10$km/s) to $\sim \pm 10$km/s or higher for very rapid rotators ($v \sin i \geq 100$km/s). Compared with Paper I, we were able to reduce the upper limit of our $v \sin i$ resolution from 10 km/s to

7 km/s. Such improved resolution of small $v \sin i$ values was the result of a more careful calibration of cross-correlation output from the template spectra in the 7-10km/s range – as performed for Hamilton observations in the Pleiades (Soderblom etal. 1993).

In Table 1 we provide a summary of the new echelle observations. After the star name, we list VBI photometry from Paper I, the measured radial velocity ($v_{\rm rad}$) and rotational velocity ($v \sin i$), notes on the presence (Y) or absence (N) of Li 6707, notes on the Hα feature, and the UT and Julian dates of observation. An 'N' is appended to the star name to flag those stars we consider to be nonmembers based on the echelle data – i.e., those having $v_{\rm rad}$ measures inconsistent with cluster membership, and/or the absence of a Li feature and Hα emission. Some comments on individual stars now follow.

The $v_{\rm rad}$ measures of HE416 from this paper and Paper I are the same within the errors of measurement, suggesting that HE416 is not a single-line spectroscopic binary as suggested previously. Although HE416 appears to have a weak Li 6707 line in our spectrum, the fact that Hα is observed in absorption, that $v_{\rm rad}$ is significantly different from the cluster mean ($v_{\rm clust} \simeq -2$km/s), and that Ca H&K are not seen in emission (Stauffer etal. 1993) all suggest that HE416 is not a cluster member. The repeat observation here of cluster member HE1181 also shows no radial velocity variation when compared to the earlier observation in Paper I.

Among the AP candidates which have been observed for the first time at high resolution, we find a mixture of slow, moderate, and rapid rotators. The $v_{\rm rad}$ and $v \sin i$ estimates for the very rapid rotators are rather uncertain because the high resolution employed results in broad, shallow absorption lines in the spectrum of these stars. Analysis of photometric periods (Prosser etal. 1993) for the rapid rotators AP139 & AP258 finds that the high $v \sin i$ values quoted for those stars (Paper I) are in error and that $v \sin i \simeq 170$km/s would be more appropriate projected rotational velocity estimates. Photometric periods have been obtained for both AP63 & AP124 and will be reported elsewhere.

2.2 Revised $v \sin i$ Upper Limits

In Paper I, $v \sin i$ values were considered measurable down to 10 km/sec. Stars which had projected rotational velocities below 10 km/s were assigned an upper limit designation of '$\leq$ 10km/s' and not analyzed further. Since then, it has been shown (Soderblom etal. 1993) that with sufficient signal-to-noise in the spectrum and with careful analysis the Hamilton echelle can achieve $v \sin i$ resolution down to $\sim$ 7km/s. We decided to reanalyze the $v \sin i$ measures for the slowly rotating candidate α Per members in Paper I in order to provide better defined measures and upper limits.

The reanalysis was performed for those possible members from Paper I which were originally listed as having $v \sin i \leq 10$km/s (or around 10 km/s). The cross-correlation analysis for determining $v \sin i$ was performed using a software package developed and provided by Rob Hewett (CfA). A high signal-to-noise spectrum of the day sky was used as a template for calibration purposes. The revised $v \sin i$ measures are given in Table 2, where we also list the previous $v \sin i$ values from Paper I. A fair number of the revised measures are seen to be < 7km/s, below the threshold of resolution with the Hamilton echelle. A spectroscopic survey at Ca H&K (Stauffer etal. 1993) has shown that all the stars with $v \sin i < 7$km/s in Table 2 can be considered as nonmembers. On the other hand, on the basis of the Ca H&K data, HE 340 and AP121 (both with $v \sin i = 7$km/s) appear to be members.

3. Photometry

3.1 New Observations

In a proper motion study, Prosser (1992, =Paper I) was able to identify candidate cluster members to V$\simeq$18.8 ($M_V \simeq 12.5$) and provided spectral types for some candidate members down to V$\sim$17 ($\sim$ M4V). As stated in Paper I, some accuracy was sacrificed in the photometry obtained for the fainter stars due to the large number of overall candidates that had to be observed. The increase in photometric errors beyond V$\simeq$17 results in an artificial widening of the V vs. V$-$I diagram of cluster members (Fig. 10, Paper I), and degrades the ability to obtain contraction ages and to compare low-mass α Per stars with similar stars in other clusters.

In an effort to overcome this, a program to obtain more accurate magnitudes and colors for the faint AP stars was begun and the first results are reported here. The observations were obtained using the 48-inch telescope at the Fred Lawrence Whipple Observatory on Mt. Hopkins, AZ. A 2048 $\times$ 2048 CCD was used, which gave a usable field of view of $\sim 9' \times 9'$ ($0.6''$/pix at 2×2 binning). The photometry was primarily obtained during Oct, Nov 1991 at which time filters had to be manually changed at the telescope. DAOPHOT (Stetson 1987) was employed to determine instrumental magnitudes using aperture photometry with annular sky value subtraction. Standard stars from Landolt (1973,1983), Joner & Taylor (1990), and Stauffer (1982) were observed each night and used for calibration. In addition to V & I_{Kron} photometry, R_{Kron} magnitudes were obtained for several α Per stars. In Table 3 we list the new V, V$-I_K$ observations along with the previous measures from Paper I. In Table 3 we also give the combined or average of the new and previous photometry, which we adopt here. The R_{Kron} photometry is given in Table 4. Because the filters had to be manually changed during this observing run, the R magnitude observations were obtained by observing program and standard stars in R only and accounting for color influences in reduction to a standard system by employing a 'V$-$r' color term; the transformation equation for R then being:

$$R = ar + b(V - r) + c$$

where,

$$R = \text{standard Kron R mag.}$$

$$r = \text{observed, instrumental r mag.}$$

$$V - r = \text{standard or known V minus instrumental r.}$$

After dropping deviant measures we found:

$$R = 0.986r - 0.344(V - r) + 2.326 \qquad (62\text{stars})$$

$$(\pm 0.005) \ (\pm 0.024) \qquad (\pm 0.061).$$

Similar transformation equations were used to obtain V & I, using ~ 40 standard stars and employing an instrumental (v−i) color term since new observations in both V & I were obtained here for these stars.

In Figure 1 we illustrate the effect of the new (V,V−I) photometry. In the top panel we show the photometry from Paper I for the low-mass members and candidate members. In the lower panel, we have replaced the photometry from Paper I with the adopted (V,V−I) values from Table 3 for those stars that have been reobserved. The cluster sequence for V>16 is seen to be noticeably better defined when the new photometry is used. The cluster sequence should be even better defined once all V>16 stars are reobserved in V & I.

In Figure 2 we provide a V vs. $V-R_K$ diagram for α Per, based on the available R photometry from Stauffer etal. (1985,1989) and the R magnitudes in Table 4. Fewer stars in the $14 < V < 16$ range are seen in this diagram than in Figure 1 because the R-band observations in Table 4 were obtained primarily for those stars with $16 < V < 18$. The (V,V−R) photometry for AP6 and AP207 place both stars away from the general cluster sequence. Both these stars have nearby close companions seen on the CCD frames which may have affected the photometry. Their (V,V−R) photometry plotted in Figure 2 was obtained using the V magnitudes from Paper I and the new R magnitudes obtained here. The V magnitudes from Paper I may be in error due to the observed nearby companions; further photometric observations of these stars are clearly warranted. Another star, AP177, is also observed to lie at a significantly bluer V−R color than other stars with similar V magnitudes. As its photometry is believed to be accurate and is not influenced by a close companion, it would appear that AP177 has photometry inconsistent with cluster membership. In fact, it was previously listed as a questionable member in Paper I on the basis of its ($V,V-I_K$) photometry.

In addition to the faint AP stars with new (V,V−I) photometry in Table 3, we also provide new photometry for a few other HE and AP stars in the cluster region. HE 828 is a visual binary consisting of stars with almost equal brightness in V. HE 828B is a very red field star lying $\sim 10.5''$ west of HE 828A. HE 828 was identified as an optical counterpart to an IRAS point source (Trullols etal. 1991); most probably the infrared emission arises from HE 828B, which like the other three stars identified by Trullols etal. as corresponding to IRAS sources, is not a cluster member. AP 22 was one of the original proper motion candidates from Stauffer etal. (1985) which lacked photometry (Table 9, Paper I). On the basis of its (V,V−I) photometry in Table 3, AP 22 does not appear to be a member.

3.2 New Photometry Candidates

As the new photometry for the faint AP stars ($V \sim 17-18$) was obtained using relatively long exposure times in order to obtain high counts and low errors in the target star magnitudes, other stars several magnitudes fainter could be measured on the same CCD frame. Accordingly, the V & I CCD images were visually blinked in order to find additional faint, red stars in the CCD field of view which might have magnitudes and colors compatible with cluster membership. A similar photometric search for very low-mass members of the Pleiades has been done by Stauffer etal. (1989,1993).

The results of this search for faint red stars is shown in Figure 3, where we plot V vs. $V-I_K$ for the faint red candidates picked out by eye and the known cluster members. The photometry of AP143C, the close companion star to AP143, was reported in Paper I. The majority of stars in Figure 3 are seen to have V−I colors which are too blue for their V magnitudes, and thus are incompatible with membership in α Per. This is not surprising given that the stars were selected from photometry only and also given the low galactic latitude for α Per ($b \sim -7°$). A small fraction of the sample appears however to have redder V−I colors than usual for a given V mag.[1] Their (V,V−I) photometry appears also to coincide with what one might predict for cluster members based on the previous known members and α Per's age. Could these be cluster members?

Photometry alone is not sufficient to determine membership. Proper motion information would probably be the best evidence for membership, along with the observed photometry. A concerted proper motion survey to this magnitude range

[1] A similar effect was seen at brighter V mags in Paper I (Figure 4), where the V−I color was seen to provide a good discrimation between cluster and field stars.

however would involve considerable effort and resources. While we would like to obtain such proper motion measures in the future, at this time we must rely on other evidence, namely low-dispersion spectra, which we describe in the next section.

In Table 5 we present a list of new candidate low-mass members of the α Persei cluster. Stars listed in this table include the photometry candidates from the present survey, along with the two newly discovered flare stars of Tsvetkov etal. (1993) and the candidate member of Rebolo etal. (1992), which was identified using photometric criterion similar to that employed in this study. Although these new candidates were selected using different criterion than were employed for the AP candidates in Paper I, they have been given 'AP' identification numbers for ease of reference, sorted by RA and consecutively numbered following the list of Paper I. Table 5 lists the star name, VRI photometry, coordinates and additional notes. Of those faint red stars measured and shown in Figure 3, only those whose (V,V−I) photometry showed them to be placed redward of the general background field and which appeared possibly consistent with cluster membership have been listed in Table 5. The coordinates were derived using the GASP software, except for those stars with 'CCD' after their position, which indicates that the position was derived using a CCD frame of the field. Stars lying near the edge of a CCD frame (within $\sim$ 100 pixels) have the note 'edge'. AP303 appears to be a close double with a separation of $\sim 1.2''$; the photometry given is of the combined pair. A few stars were too faint to allow reliable V magnitudes to be measured and upper limits in V have been given. In a few cases, the quoted magnitudes are given with less precision when warranted. The location in the (V,V−I) diagram of the selected candidates in Table 5 is shown in Figure 4. Like the earlier AP lists (Stauffer etal. 1985,1989; Prosser 1992) not all are expected to be members, but hopefully the stars listed in Table 5 will be the source for the discovery of new low-mass members. Finding charts for these candidates are provided in Appendix B.

Of the new candidates originally chosen as having photometry acceptable for cluster membership, one star was subsequently identified as a high proper motion star from comparison of its positions on CCD frames taken in 1991 and on the Palomar Schmidt (POSS-I) scans obtained using the GASP software at STScI. Clearly a proper motion nonmember, it has been given the designation 'HPM 9' to follow the earlier list of new high proper motion stars discovered in the α Per region (Prosser 1990). Spectroscopic observation (to be described in the next section) finds HPM 9 to be a late-type M dwarf without any evidence of Hα emission.

4. Low-Dispersion Spectra.

In a cluster as young as α Per[1], one would predict that the low-mass stars will exhibit Hα in emission (Stauffer etal. 1984, Herbig 1985). Low-dispersion spectra at Hα were used in Paper I to aid in confirming membership by the presence of Hα emission and by the possession of a spectral type compatible with membership. We employ the same technique here to investigate the nature of some of the new faint, red photometry candidates described in the last section.

Spectra having a dispersion of ~ 1.7 Å/pix were obtained with the new Kast Spectrograph at the Lick Observatory 3m telescope, using red grating #3 with blaze at 8460Å. The spectra were used to a) detect Hα emission and b) determine spectral types from the calibration of molecular band (e.g. TiO) strengths. Spectral types were estimated using an index calibration similar to that used before in α Per and the Pleiades (Prosser etal. 1991, Prosser 1992). Table 6 lists the spectral regions defining the indices, the spectral type calibration being based essentially on the relative strengths of TiO bands. Table 7 lists the MK standard stars (Keenan & McNeil 1976) observed and used to transform the index values measured to a spectral type; for M6 and later, two stars from the list of Kirkpatrick etal. (1991, =KHM) were observed. For GL 411, the M2 V classification from KHM was employed since it appeared to provide a somewhat better calibration than the original M2.5 V MK determination.

Based on the indices measured as defined in Table 6, the following index ratios were formed: $R_3/R_7, R_3'/R_7, R_4/R_7, R_8/R_7$, and R_8/R_9. The R_6/R_5 ratio, previously used for early M dwarfs in α Per and the Pleiades, was found to be a poor calibration index for very late spectral types ($\geq$ M5), probably due to saturation of the TiO band measured by the R_6 index, and was not used further. After calibration of each of the above index ratios with the spectral type standards in Table 7, corresponding spectral types were computed from each index ratio for the candidates observed. A 'final' spectral type was obtained by averaging the spectral types from the five index ratios above, using equal weighting. The derived spectral types, refered to as pseudo-MK (or 'pMK') spectral types, are believed to be good to $\sim \pm 0.5$ in spectral type subclass. AP282 was observed separately by J. Stauffer at the MMT; the spectrum is that of an M dwarf and does not show Hα emission. In Table 8 we provide the results of the Kast observations, listing the candidate observed, the derived pMK spectral type, an indication of whether or not Hα emission was observed in the spectrum, and a measure of the Hα emission equivalent width. Sample Kast spectra for some stars are shown

[1] Generally acknowledged to be younger than the Pleiades, the exact age of the α Persei cluster is a matter of some debate. Ages from $\sim 5 \times 10^7$ to $7 - 8 \times 10^7$ yrs are quoted in the literature. The author tends at the present time to favor the slightly older age estimate (Paper I).

in Figure 5.

In Figure 6 we show the photometrically selected sample and indicate those stars which did and did not show Hα emission. Limited telescope time and the desire to possibly establish a sequence of candidate cluster members over the range $18 < V < 21$ influenced the selection of candidates observed at Hα. Those stars which were among the reddest at their V mags and which thus appear to have the best chance of being cluster members were predominantly observed. Of the photometric sample, not many stars which fall below the general location of cluster members in Figures 3 & 6 are expected to have Hα in emission; in Paper I several of the photometric nonmembers falling below the cluster sequence were observed spectroscopically and only in one case was Hα emission detected.

One of the faintest photometric candidates indicated as showing Hα emission in Figure 6 is the 'brown dwarf' candidate Ap $0323 + 4853$ (Rebolo etal. 1992) for which (V,V$-$I) photometry was obtained here in Nov. 1992. While Ap $0323 + 4853$ may indeed by a cluster member, evidence in support of its actually being a brown dwarf member is somewhat meager at present and we prefer to wait until additional data on this interesting object becomes available before discussing it further.

A few (three out of 11 observed here) stars in Figure 6 are seen to have Hα in absorption and thus are not likely to be cluster members. This is not surprising given the high field star density in the α Per region and the fact that the current candidates were selected by photometry alone. Several of the reddest candidates however are seen to exhibit Hα emission and would appear to form a natural extension to the cluster sequence established in Paper I. We note that the Hα emission stars also appear to form an extension of the cluster sequence if plotted in a V vs. pMK spectral type diagram, such as Fig. 6 of Paper I. All candidates are M dwarfs of spectral type M3 or later. The CaH absorption bands at 6385Å and 6909/6946Å, normally used as a M dwarf indicator (Turnshek etal. 1985), are seen to be present in the spectra of Figure 5.

5. Discussion

We have aimed to refine our knowledge of the lower main-sequence and pre-main sequence of α Per through spectroscopic and photometric observations. First time echelle spectroscopy of 13 AP stars has enabled the identification of three non-members and a variety of slow and fast rotating members amongst the remaining candidates. Repeated observation of HE416 suggests that this star is a nonmember. Revised $v \sin i$ estimates have been provided for several of the slow rotator candidate members of Paper I. All stars with $v \sin i < 7$ km/s are considered to be nonmembers based on Ca H&K observations reported elsewhere (Stauffer etal. 1993). Two stars however, AP121 and HE340, are found with $v \sin i = 7$ km/s and are perhaps the slowest rotating members currently known on α Per's lower main sequence. The existence of such slow rotating members can provide observational constraints on the timescale for evolution of the angular momentum distribution of a cluster population. To this end, it would be prudent to confirm that these stars are in fact single stars.

New (V,V−I) photometry has been obtained for several of the fainter AP stars. Application of the new photometry shows an improvement in the definition of the cluster pre-main sequence. When all such faint members have improved photometry, it should enable one to make better age estimates and better identification of photometric binaries. R-band photometry has been obtained for several stars in an effort to provide more complete photometric coverage and better comparison to other open clusters.

The new CCD photometry obtained for previous cluster members has formed the basis for a search for new candidate low-mass members on the basis of their photometry. Of the $\sim$ 43 new photometric candidates presented, low-dispersion spectra at Hα have identified three nonmembers by their lack of Hα emission and provided supporting evidence for cluster membership for another eight stars with Hα emission. The new candidates observed with Hα emission appear to form a natural extension of the cluster membership down to V $\simeq$ 21. The latest spectral type derived among the new candidates is $\sim$ M5.5. The new AP candidates have a less well-founded membership status than the earlier AP star samples which resulted from color-selected, proper motion surveys. Yet, the V−I color appears to be an efficient discriminator between cluster & field stars, and a photometrically-selected sample by itself can provide a means to extend the cluster membership until proper motion surveys at such faint magnitudes can be undertaken.

In addition to proper motion information, it would be advisable to obtain low-dispersion spectra at longer wavelengths and infrared photometry (particularly K-band) of the new photometric candidates to assess membership. A system of spectral classification in the red/near-infrared such as that described in KHM would provide a means to construct a spectral sequence for an ensemble of stars of the same age and metallicity. Such a spectral classification in a cluster like Alpha Per would enable one to study spectral characteristics for very low-mass stars without the complications of metallicity/age effects encountered in a random field sample. A careful calibration of the spectral type vs. mass and spectral type vs. temperature relations using nearby stars would in turn yield much desired mass and temperature estimates for the low-mass cluster stars.

We gratefully acknowledge the assistance of Rob Hewett for providing the software using in the $v \sin i$ reanalysis described in section 2.2. We would like to acknowledge the assistance of the staff of Lick Observatory, particularly Rem Stone and Tony Misch who assisted in our instrument configurations. Tony Misch obtained echelle observations in service observing for part of this program in August 1991. Astrometry obtained using the Guide Stars Selection System Astrometric Support Program (GASP) developed at the Space Telescope Science Institute (STScI is operated by the Association of Universities for Research in Astronomy, Inc. for NASA). The helpful assistance by Dan Golombek and Kerry McQuade at STScI during a visit to STScI is acknowledged. The new flare star identifications were kindly provided in advance of publication by M. Tsvetkov, E. Semkov, and K. Tsvetkova. The author acknowledges Bob Kraft, who provided continuing assistance and comments on this program, and Burt Jones, who originally brought to the author's attention the prospects of an extensive membership survey in the α Persei cluster. This study was supported by NASA Grant No. NAGW-2698 (to J. Stauffer).

Appendix A

In this appendix we present a revised set of coordinates for the AP stars originally reported in Paper I. The 2000 coordinates listed in Table A1 were obtained using the GASP software at STScI. The digitized scans of the Palomar Observatory Sky Survey (POSS-I) E plates were employed, since many of the AP stars are most easily measurable and identifiable in the red. The resulting coordinates will be slightly less accurate than if the 'Quick V' scans used in constructing the HST Guide Star Catalog had been used, but the measured coordinates should still be accurate to within an arcsecond or slightly better.

The original 1950 coordinates reported in Paper I for these stars were obtained after fitting a plate solution to the positions of various SAO stars located over the field of the Schmidt plate. Subsequent use showed deviations from the calculated positions, particularly as a function of declination. When the new positions are compared to the original positions in Paper I, the deviations in declination values between the new and old positions are found to noticeably increase for stars at declinations below $+48^{\circ}$. The deviations are on the order of $10''$ for the southernmost stars, in the sense that the old positions placed the star further to the north than it actually was. The new GASP positions will be useful in future membership surveys and in projects involving comparison of x-ray or radio source information to optical identifications.

Appendix B

Finding charts are provided here for those new AP stars listed in Table 5; the new photometric candidates of this study along with the couple of new candidate members identified in Tsvetkov etal. (1993) and Rebolo etal. (1992). The charts are constructed from the original I-band CCD discovery images. The field shown in the charts is $1.5' \times 1.5'$, with north up and east to the left.

References

Heckmann, V.O., Dieckvoss, W. and Kox, H. 1956, Astr. Nach. 283, 109

Heckmann, V.O. and Lübeck, K. 1958, Zeitschrift für Astrophysik 45, 243

Herbig, G.H. 1985, ApJ 289, 269

Joner, M.D. and Taylor, B.J. 1990, PASP 102, 1004

Keenan, P.C. and McNeil, R.C. 1976, 'An Atlas of Spectra of the Cooler Stars: Types G,K,M,S, and C' (Columbus: Ohio State University Press)

Kirkpatrick, J.D., Henry, T.J., and McCarthy, D.W. Jr. 1991, ApJS 77, 417

Landolt, A.U. 1973, AJ 78, 959

Landolt, A.U. 1983, AJ 88, 439

Mitchell, R.I. 1960, ApJ 132, 68

Petrie, R.M. and Heard, J.F. 1970, Pub. of the Dominion Astrophysical Obs. 13, 329

Prosser, C.F. 1990, PASP 102, 96 (Lick Obs. Bull. 1152)

Prosser, C.F. 1992, AJ 103, 488 (Paper I) (Lick Obs. Bull. 1201)

Prosser, C.F., Stauffer, J.R., and Kraft, R.P. 1991, AJ 101, 1361

Prosser, C.F., Schild, R.E., Stauffer, J.R., and Jones, B.F. 1993, PASP 105, 269

Rebolo, R., Martín, E.L., and Magazzù, A. 1992, ApJL 389, 83

Soderblom, D.R., Pendleton, J., and Pallavicini, R. 1989, AJ 97, 539

Soderblom, D.R., Stauffer, J.R., Hudon, J.D., and Jones, B.F. 1993, ApJS 85, 315

Stauffer, J.R. 1982, AJ 87, 899

Stauffer, J.R. and Hartmann, L.W., Soderblom, D.R., and Burnham, N. 1984, ApJ 280, 202

Stauffer, J.R. and Hartmann, L.W., Burnham, J.N., and Jones, B.F. 1985, ApJ 289, 247

Stauffer, J.R., Hartmann, L.W., and Jones, B.F. 1989, ApJ 346, 160

Stauffer, J.R., Hamilton, D., Probst, R., Rieke, G., Mateo, M. 1989, ApJL 344, 21

Stauffer, J.R., Prosser, C.F., Giampapa, M.S., Soderblom, D.R., and Simon, T. 1993, AJ, in press

Stauffer etal. 1993, in preparation

Stetson, P.B. 1987, PASP 99, 191

Trullols, E., Rosselló, G., Jordi, C., and Lahulla, F. 1989, A&AS 81, 47

Trullols, E., Jorki, C., and Rosselló, G. 1991, in 'The Infrared Spectral Region of Stars', edited by C. Jaschek and Y. Andrillat (University Press, Cambridge), p. 38.

Tsvetkov, M., Semkov, E., Tsvetkova, K., and Prosser, C. 1993, submitted to IBVS

Turnshek, D.E., Turnshek, D.A., Craine, E.R., and Boeshaar, P.C. 1985, An Atlas of Digital Spectra of Cool Stars (Tucson: Western Research Co.)

Vogt, S.S. 1987, PASP 99, 621

Figure Captions

Figure 1. The (V,$V-I_K$) photometry of members and candidate members from Paper I (top panel) is compared to the same color magnitude diagram when the new photometry from Table 3 for stars with $V > 16$ is substituted (bottom panel). The cluster sequence is seen to be better defined by the new observations.

Figure 2. V vs. $V-R_K$ diagram for α Per members and candidate members. See the text for a discussion on the possible reasons for the positions of the three stars noted.

Figure 3. V vs. $V-I_K$ diagram showing the photometric sample of stars originally selected as possible candidate members based on their appearence as very red stars on CCD frames. The location of known cluster members from Paper I are shown. While most of the new photometry candidates are seen to not have (V,$V-I$) photometry compatible with membership, some of the very reddest stars observed at a given V may be considered to have photometry that is in accordance with membership in the cluster.

Figure 4. Same as Figure 3, but with those stars selected as having photometry acceptable with membership now indicated. The flare stars from Tstvekov etal and the candidate member from Rebolo etal. are also included in the selected candidate group.

Figure 5. Sample Kast spectra at Hα for some of the new photometry candidates listed in Table 5.

Figure 6. The sample of new photometry candidates as in Figure 3, with those stars observed to have Hα in emission or absorption indicated. The brightest new candidate member indicated as having Hα emission is a flare star discovered by Tsvetkov etal. (1993), while one of the faintest stars seen with emission is the faint 'brown dwarf' candidate member of Rebolo etal. (1992) and is plotted as a solid triangle. The observed Hα emission and pMK spectral types obtained for the new candidates is suggestive of the existence of a cluster sequence extending to $V \sim 21$, though additional evidence to more fully confirm membership for the photometry candidates is needed.

TABLE 1. New Echelle Observations

Star	V	B−V	V−I	$v_{\rm rad}$ (km/s)	$v \sin i$ (km/s)	Li	Hα	UT Date	Julian Date (JD. - 2448000.0)
HE 116N	10.85	0.68		+9.3 (±0.8)	< 7	Y(wk.)	absorp.	Nov 15, 91	575.730
HE1181	10.57	0.58	0.49	−4.7 (±0.8)	< 7	Y	absorp.	Nov 16, 91	576.615
AP 63	12.29	0.92	0.84	+9.9 (±12)	161:	–	emiss?	Aug 21, 91	489.928
AP124	13.44		1.25	—	190:	Y	emiss.	Nov 15, 91	575.822
AP137N	13.38		1.18	+8.6 (±0.8)	< 7	N	absorp.	Nov 16, 91	576.943
AP158	11.93	0.85	0.82	−3.0 (±1.0)	15	Y	absorp.	Aug 21, 91	489.889
AP167	13.52		1.20	−4.4 (±13)	96:	Y	emiss.	Nov 16, 91	576.781
AP169	13.28		1.07	−0.4 (±0.8)	10	Y(wk.)	wk. absorp.	Nov 16, 91	576.899
AP189	13.05	0.94	0.99	−2.4 (±7.5)	92:	Y	emiss.	Nov 15, 91	575.767
AP212	13.24		0.97	−0.9 (±0.8)	12	Y(wk.)	wk. absorp.	Nov 16, 91	576.983
AP231	14.07		1.29	−0.1 (±1.2)	25	Y(wk.)	emiss.	Nov 16, 91	576.839
AP247	13.20		0.97	+0.3 (±1.0)	20	Y	emiss.	Aug 21, 91	490.010
AP249N	13.37		1.20	+6.2 (±0.8)	12	N	absorp.	Nov 16, 91	576.732
AP257	13.00		0.92	+0.7 (±0.8)	11	Y	filled	Nov 16, 91	576.644
AP263N	13.21	1.19	1.11	+30.3 (±1.0)	< 7	N	absorp.	Nov 16, 91	576.687

TABLE 2. New $v \sin i$ Measures

STAR	Paper I Membership[1]	Paper I $v \sin i$[1] (km/s)	Revised $v \sin i$ (km/s)	Ca H&K Membership[2]	Current Membership
HE 56	Y	< 10	< 7	N	N
HE 143	Y	< 10	< 7	N	N
HE 340	Y?	< 10	7	Y	Y
HE 347	Y?	< 10	< 7	N	N
HE 416	Y?	< 10	< 7	N	N
HE 992	Y?	< 10	14		Y?
HE1086	Y	12	12		Y
HE1100	Y	< 10	8		Y
HE1110	Y?	< 10	< 7	N	N
HE1181	Y	< 10	< 7	N	N
HE1185	Y	< 10	11		Y
HE1234	Y	10	10		Y
AP 121	Y	< 10	7	Y	Y
AP 156	Y	< 10	8		Y
AP 168	?	< 10	< 7	N	N
AP 194	Y	< 10	< 7	N	N
AP 195[3]	Y?	< 10	< 7	N	N
AP 222	?	< 10	9		?
AP 255	Y	< 10	< 7	N	N

[1]Prosser (1992).

[2]Stauffer etal. (1993).

[3]two observations of this star, 12/18/89 and 12/10/90, yield identitical $v \sin i$ results.

TABLE 3. (V,V-I) Photometry of α Per Stars

Star	New		Paper I		Difference		Combined	
	V	$V-I_K$	V	$V-I_K$	ΔV	$\Delta V-I_K$	V	$V-I_K$
AP123	16.35	2.40	16.28	2.20	+0.07	+0.20	16.31	2.30
AP126	16.60	2.52	16.57	2.40	+0.03	+0.12	16.58	2.46
AP128	16.91	2.69	16.96	2.60	−0.05	+0.09	16.93	2.65
AP132	17.08	2.91	17.22	2.88	−0.14	+0.03	17.15	2.90
AP133	17.59	2.89	17.57	2.71	+0.02	+0.18	17.58	2.80
AP135	17.76	2.93	17.72	2.79	+0.04	+0.14	17.74	2.86
AP136	17.14	2.77	17.07	2.58	+0.07	+0.19	17.10	2.68
AP141	18.16	3.22	18.19	3.12	−0.03	+0.10	18.17	3.17
AP146	16.36	2.46	16.40	2.37	−0.04	+0.09	16.38	2.42
AP147	17.06	2.77	17.19	2.76	−0.13	+0.01	17.12	2.77
AP148	17.84	3.01	17.71	2.84	+0.13	+0.17	17.77	2.92
AP152	18.29	3.01	18.15	2.82	+0.14	+0.19	18.22	2.91
AP157	17.17	2.97	17.07	2.78	+0.10	+0.19	17.12	2.87
AP159	17.90	3.05	17.88	2.91	+0.02	+0.14	17.89	2.98
AP161	14.83	2.05	14.95	2.07	−0.12	−0.02	14.89	2.06
AP164	17.25	3.12	17.22	2.97	+0.03	+0.15	17.23	3.05
AP165	17.11	2.66	17.24	2.58	−0.13	+0.08	17.17	2.62
AP180	16.28	2.46	16.34	2.41	−0.06	+0.05	16.31	2.44
AP182	17.29	2.82	17.32	2.70	−0.03	+0.12	17.30	2.76
AP186	17.12	2.43	17.33	2.51	−0.21	−0.08	17.22	2.47
AP192	18.36	2.75	18.40	2.70	−0.04	+0.05	18.38	2.73
AP204	17.25	2.70	17.17	2.50	+0.08	+0.20	17.21	2.60
AP209	16.33	2.25	16.41	2.22	−0.08	+0.03	16.37	2.24
AP219	16.50	2.34	16.58	2.23	−0.08	+0.11	16.54	2.29
AP234	18.36	2.84	18.39	2.72	−0.03	+0.12	18.37	2.78
AP236	17.37	2.80	17.32	2.64	+0.05	+0.16	17.34	2.72
AP238	14.29	1.73	14.25	1.66	+0.04	+0.07	14.27	1.69
AP239	16.35	2.27	16.39	2.20	−0.04	+0.07	16.37	2.24
AP240	17.17	3.21	17.15	3.06	+0.02	+0.15	17.16	3.14
AP243	18.39	2.82	18.44	2.82	−0.05	+0.00	18.41	2.82
AP251	18.31	2.99	18.29	2.87	+0.02	+0.12	18.30	2.93
AP253	18.19	2.96	18.08	2.76	+0.11	+0.20	18.13	2.86
AP262	18.57	2.95	18.60	2.87	−0.03	+0.08	18.58	2.91
AP265	17.56	2.88	17.48	2.66	+0.08	+0.22	17.52	2.77
HE828A	11.62	0.64					11.62	0.64
HE828B	11.88	2.83					11.88	2.83
HE833	10.06	0.40					10.06	0.40
HE848	10.00	0.50	10.00	0.46	+0.00	+0.04	10.00	0.48
AP 22	16.90	2.33					16.90	2.33

TABLE 4. R(Kron) Photometry of AP Stars

Star	R_K	$V-R_K$	Star	R_K	$V-R_K$
AP 6	14.75	0.78	AP148	16.32	1.45
AP 6C	15.92	1.92	AP150	15.59	1.34
AP 8	15.45	1.29	AP151	15.91	1.39
AP 15	13.38	0.74	AP152	16.74	1.48
AP 16	14.90	1.13	AP153	16.41	1.55
AP 17	14.19	1.09	AP154	16.03	1.74
AP 18N	16.35	-0.15	AP155	15.31	1.49
AP 20	14.34	1.32	AP157	15.64	1.53
AP 21	14.37	1.20	AP159	16.22	1.67
AP 22N	15.61	1.29	AP160	17.10	1.73
AP 27N	16.01	0.45	AP161	13.65	1.24
AP 29N	14.98	0.95	AP162	15.59	1.50
AP 34	14.98	1.22	AP163	16.69	2.12
AP 56	12.46	0.54	AP164	15.61	1.62
AP 60	14.40	1.34	AP165	15.70	1.47
AP 84N	16.41	-0.21	AP170	16.37	2.05
AP 86	13.23	1.08	AP171	14.59	1.16
AP 92	14.49	1.17	AP172	15.15	1.35
AP 96	13.33	1.22	AP174	13.95	1.36
AP 99	14.59	1.09	AP175	15.86	1.59
AP103	14.46	1.30	AP176	14.98	1.43
AP107	16.30	2.23	AP177	17.23	1.37
AP109	14.68	1.16	AP178	15.47	1.42
AP120	13.82	1.36	AP179	15.26	1.51
AP122	14.01	1.17	AP180	14.99	1.32
AP123	15.06	1.25	AP181	15.99	1.61
AP126	15.23	1.35	AP182	15.80	1.50
AP128	15.52	1.41	AP183	14.66	1.16
AP129	14.41	1.50	AP184	15.19	1.31
AP131	14.78	1.34	AP185	15.11	1.34
AP132	15.63	1.52	AP186	15.78	1.44
AP133	16.10	1.48	AP187	15.28	1.21
AP134	14.84	1.25	AP188	13.50	0.85
AP135	16.22	1.52	AP190	17.30	—
AP136	15.69	1.41	AP191	14.33	1.30
AP138	13.58	0.98	AP192	16.91	1.47
AP140	14.65	1.31	AP198	14.09	1.25
AP141	16.48	1.69	AP202	14.06	1.14
AP142	14.52	1.22	AP203	16.35	1.75
AP143	16.12	1.88	AP204	15.83	1.38
AP143C	17.68	2.24	AP205	14.00	1.20
AP144	13.37	1.00	AP207	15.35	0.92
AP145	15.20	1.50	AP208	14.19	1.35
AP146	15.06	1.32	AP209	15.11	1.26
AP147	15.66	1.46	AP210	14.66	1.30

TABLE 5. New Photometry Candidates

AP	V	$V-I_K$	$V-R_K$	$R-I_K$	RA (2000)	DEC		Notes
267	17.93	2.99	1.69	1.30	3 17 54.146	49 28 23.92		edge
268	21.81:	4.40	2.02	2.38	3 18 09.31	49 25 17.4	CCD	V upper limit
269	20.42	3.72	2.19	1.53	3 19 47.647	48 58 44.07		
270	17.88	3.05	1.54	1.51	3 20 43.002	51 01 08.06		edge
271	21.78	4.20	2.40	1.80	3 20 43.85	50 59 37.0	CCD	edge
272	22.23	4.27	2.94	1.33	3 21 02.50	47 27 27.5	CCD	
273	16.34	2.21	1.23	0.98	3 21 06.689	47 24 31.31		
274	19.99	3.53	2.17	1.36	3 21 26.888	49 48 04.72		
275	20.34	3.88	2.20	1.68	3 21 43.010	49 48 36.06		
276	21.51	3.81	2.28	1.53	3 22 39.49	47 28 14.8	CCD	
277	21.62	4.10	2.69	1.41	3 22 39.50	47 28 20.0	CCD	
278	23.27:	5.11:	3.85:	1.26	3 22 43.01	47 32 24.8	CCD	V upper limit
279	18.2	3.12			3 22 54.244	48 49 44.61		
280	21.1	3.95			3 23 03.344	48 53 11.27		= Ap 0323 + 4853[1]
281	21.6	3.90			3 23 19.079	48 55 10.01		
282	18.46	3.02	1.71	1.31	3 23 19.637	47 56 29.36		
283	18.97	3.27	2.04	1.23	3 23 26.932	47 52 12.25		
284	21.1	3.86			3 23 28.515	48 48 23.60		
285	19.78	3.48	2.35	1.13	3 23 31.577	47 51 28.79		
286	17.92	2.76	1.57	1.19	3 23 44.846	47 54 25.42		edge
287	17.56	2.95	1.54	1.41	3 23 46.581	47 59 20.48		edge
288	21.32	4.03	2.41	1.62	3 24 17.82	48 23 53.7	CCD	
289	18.42	3.10	1.63	1.47	3 24 22.550	48 24 26.17		
290	18.96	3.15	1.71	1.44	3 24 38.832	48 17 16.97		
291	21.99:	4.01:	2.14:	1.87	3 25 03.95	48 49 57.6	CCD	V upper limit
292	18.28	3.04	1.72	1.32	3 27 02.843	49 41 09.97		edge
293	19.38	3.48	2.00	1.48	3 27 05.592	47 25 29.71		edge
294	17.8	2.8			3 27 12.18	48 03 40.7	CCD	
295	18.7	3.4			3 27 18.09	47 57 27.3	CCD	= FS2[2]
296	20.91	3.71	2.30	1.41	3 27 29.03	47 28 53.1	CCD	
297	19.6	3.6			3 27 34.84	47 57 14.4	CCD	
298	17.12	2.71	1.46	1.25	3 27 39.948	47 29 27.29		
299	19.9	3.34			3 28 28.97	50 14 53.6	CCD	
300	19.2	3.38			3 28 29.22	50 18 08.8	CCD	
301	19.8	3.41			3 28 53.14	50 19 24.3	CCD	
302	16.17	2.26			3 28 54.416	50 16 17.80		= FS1[2]
303	18.95	3.27	1.72	1.55	3 30 47.741	48 13 00.46		close double, 1.2″
304	16.79	2.33	1.24	1.09	3 30 53.645	48 14 44.04		
305	17.59	3.05	1.56	1.49	3 31 53.411	47 20 40.09		
306	19.47	3.39	1.86	1.53	3 32 27.738	47 20 56.09		
307	18.51	3.31			3 35 40.43	48 26 26.6	CCD	nearby star
308	17.58	2.89			3 35 55.729	48 26 41.57		
309	19.06	3.07			3 37 48.050	46 36 44.51		nearby star
HPM9	16.80	2.82			3 36 09.346	48 26 18.49		edge

1. Rebolo etal. 1992.
2. Tsvetkov etal. 1993.

TABLE 6. Spectral Indice Regions

Region	Boundary (Å)
R5	6096 – 6144
R6	6170 – 6210
R3	6635 – 6718
R4	6750 – 6844
R3′	6650 – 6844
R7	7000 – 7050
R8	7062 – 7170
R9	7390 – 7490

TABLE 7. Spectral Type Standards

Star	Spt. Type	Note
GL 820A	K5 V	
GL 820B	K7 V	
GL 846	M0.5 V	
GL 411	M2 V	KHM (M2.5 MK)
GL 896B	M4 V	
GL 268	M4.5 V	
GL 83.1	M5 V	
G 208-44	M5.5 V	
G 208-45	M6 V	KHM
G 51-15	M6.5 V	KHM

TABLE 8. Spectroscopic Data

Star	pMK SPT	Hα	Hα EW (Å)
AP269	M 5.2	Y	4.2
AP275	M 5.6	Y	13.5
AP279	M 4.6	Y	4.8
AP282	–	N	–
AP284	M 5.0	Y	5.2
AP293	M 4.6	Y	5.4
AP298	M 3.3	Y	4.8
AP305	M 4.4	N	–
AP307	M 4.7	Y	6.2
AP308	M 3.9	Y	6.8
HPM 9	M 4.4	N	–

TABLE A1. GASP Coordinates for AP Stars

AP	RA (2000)	DEC	AP	RA (2000)	DEC	AP	RA (2000)	DEC
119	3 17 31.379	48 51 52.48	169	3 28 23.723	47 36 50.71	219	3 35 40.148	48 24 02.51
120	3 17 38.023	49 54 49.10	170	3 28 50.029	48 07 38.08	220	3 35 44.134	49 06 07.70
121	3 17 42.086	49 01 47.68	171	3 28 57.195	49 34 02.64	221	3 36 02.741	46 42 57.97
122	3 18 08.549	49 18 56.19	172	3 29 12.969	50 08 06.19	222	3 36 11.766	49 44 11.92
123	3 18 23.132	49 28 03.42	173	3 29 14.126	49 41 17.68	223	3 36 10.766	45 56 13.54
124	3 18 58.667	48 50 43.50	174	3 29 14.664	48 10 52.44	224	3 36 18.984	48 38 03.56
125	3 19 45.640	50 08 35.88	175	3 29 15.474	47 53 32.85	225	3 36 21.996	49 09 21.21
126	3 19 57.281	49 04 22.49	176	3 29 18.955	46 07 28.09	226	3 36 53.672	48 23 58.71
127	3 20 01.284	46 53 02.01	177	3 29 42.417	46 24 23.81	227	3 37 01.588	48 13 22.50
128	3 20 12.091	48 56 41.99	178	3 30 04.767	49 15 36.06	228	3 37 14.671	50 26 26.66
129	3 20 16.229	48 09 18.43	179	3 30 11.068	48 08 13.70	229	3 37 27.437	47 33 44.46
130	3 20 27.732	48 58 21.21	180	3 30 24.336	46 35 56.83	230	3 37 34.549	47 31 52.31
131	3 20 56.520	49 20 43.91	181	3 30 29.666	49 01 29.85	231	3 37 49.343	48 01 17.74
132	3 21 02.370	49 47 04.16	182	3 30 36.465	48 15 29.78	232	3 37 50.634	45 56 25.48
133	3 21 12.187	50 59 08.13	183	3 30 56.780	50 00 51.23	233	3 37 58.178	45 43 47.60
134	3 21 20.466	47 53 16.30	184	3 30 55.245	48 39 23.45	234	3 38 05.651	46 33 57.78
135	3 21 22.386	47 25 54.10	185	3 30 55.837	46 48 21.73	235	3 38 14.708	45 51 03.98
136	3 21 38.319	49 48 56.81	186	3 31 05.021	48 16 25.01	236	3 38 30.265	48 19 12.82
137	3 21 45.047	46 48 16.39	187	3 31 16.482	49 33 04.05	237	3 38 35.991	47 05 36.97
138	3 22 00.068	48 23 50.06	188	3 31 24.293	50 12 28.11	238	3 38 43.371	48 02 26.08
139	3 22 06.797	47 34 07.52	189	3 31 44.855	49 33 04.41	239	3 38 49.194	48 08 44.08
140	3 22 09.727	48 34 03.00	190	3 31 48.797	48 53 30.11	240	3 38 55.412	48 14 17.27
141	3 22 24.158	47 32 12.66	191	3 31 51.671	49 20 01.18	241	3 39 05.911	47 44 44.21
142	3 22 28.037	48 49 40.05	192	3 32 03.843	47 21 57.82	242	3 39 17.157	49 38 03.28
143	3 22 32.714	49 11 17.17	193	3 32 10.199	49 08 29.40	243	3 39 45.925	46 07 47.34
144	3 22 36.807	47 09 11.87	194	3 32 14.930	46 39 23.29	244	3 40 33.886	48 04 36.23
145	3 22 48.392	49 39 23.71	195	3 32 20.839	48 41 05.31	245	3 40 43.173	49 28 21.94
146	3 23 11.899	47 54 35.67	196	3 32 19.302	47 04 27.55	246	3 40 50.490	50 57 55.78
147	3 23 25.043	47 54 38.70	197	3 32 29.096	47 38 21.42	247	3 40 58.216	47 02 37.57
148	3 24 22.702	48 20 01.90	198	3 32 45.112	50 05 16.29	248	3 41 04.734	49 09 33.04
149	3 24 48.344	48 53 20.55	199	3 32 44.403	47 41 35.80	249	3 41 07.469	49 07 55.37
150	3 24 48.027	47 13 09.77	200	3 32 51.150	50 07 07.15	250	3 41 10.536	46 32 27.21
151	3 25 03.203	49 06 43.11	201	3 32 51.061	49 50 44.40	251	3 41 11.178	46 00 49.94
152	3 25 22.914	48 46 57.03	202	3 33 09.407	50 50 43.71	252	3 41 13.450	45 48 02.95
153	3 25 41.808	51 18 23.03	203	3 33 25.570	48 20 13.30	253	3 41 30.623	46 09 35.67
154	3 25 57.357	47 43 53.78	204	3 33 35.315	49 02 14.13	254	3 42 27.413	46 31 49.10
155	3 26 01.278	48 39 10.78	205	3 33 34.094	46 07 26.25	255	3 42 44.587	49 39 01.19
156	3 26 22.612	47 16 10.34	206	3 33 42.113	47 20 49.12	256	3 43 38.481	46 03 48.47
157	3 26 28.407	49 41 29.97	207	3 33 49.880	49 09 35.16	257	3 44 02.575	48 39 59.10
158	3 26 33.705	50 13 54.99	208	3 33 47.118	47 35 31.69	258	3 45 43.387	46 18 05.01
159	3 26 36.678	49 38 13.25	209	3 33 50.344	48 55 40.04	259	3 46 32.718	48 45 52.20
160	3 26 39.787	46 28 00.91	210	3 34 11.188	51 27 52.35	260	3 47 09.624	47 48 23.66
161	3 27 18.851	47 25 25.14	211	3 34 11.272	49 50 26.92	261	3 47 14.595	45 38 27.70
162	3 27 43.414	50 48 58.05	212	3 34 29.319	49 21 44.07	262	3 48 11.992	50 54 46.26
163	3 27 49.901	48 04 45.88	213	3 34 39.427	48 18 43.68	263	3 49 26.959	45 42 49.33
164	3 27 49.267	47 27 34.52	214	3 34 54.751	48 41 19.72	264	3 50 27.796	47 49 05.49
165	3 28 03.048	50 40 19.63	215	3 35 19.986	48 54 39.45	265	3 50 37.027	48 12 31.66
166	3 28 06.961	46 21 16.83	216	3 35 18.806	47 56 05.86	266	3 50 36.512	45 46 11.08
167	3 28 10.487	47 25 27.20	217	3 35 15.741	46 05 40.42			
168	3 28 19.453	45 47 49.98	218	3 35 27.798	46 44 10.45			

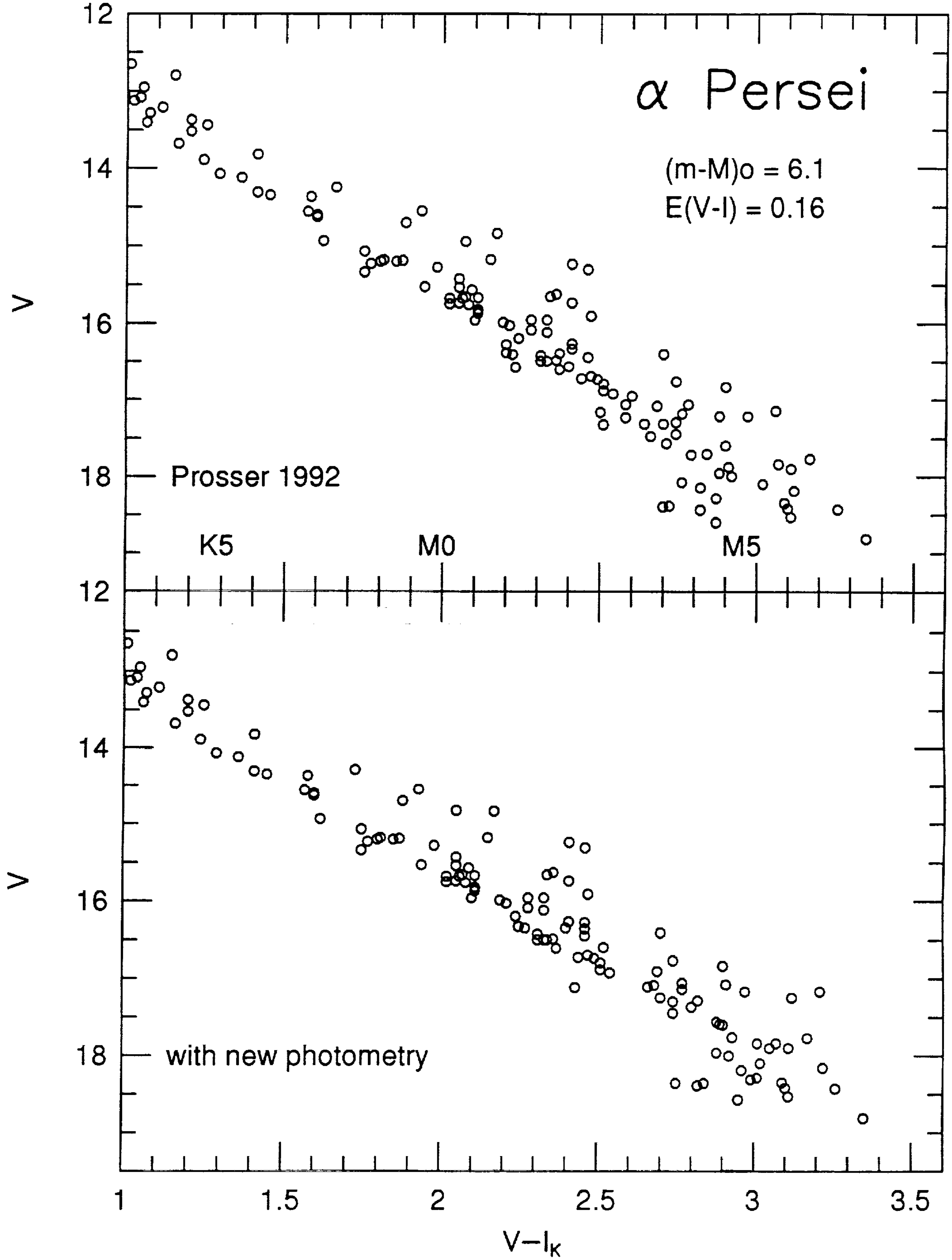
α Persei
(m-M)o = 6.1
E(V-I) = 0.16
Prosser 1992
K5
M0
M5
with new photometry
V
V−I_K
12
14
16
18
1
1.5
2
2.5
3
3.5

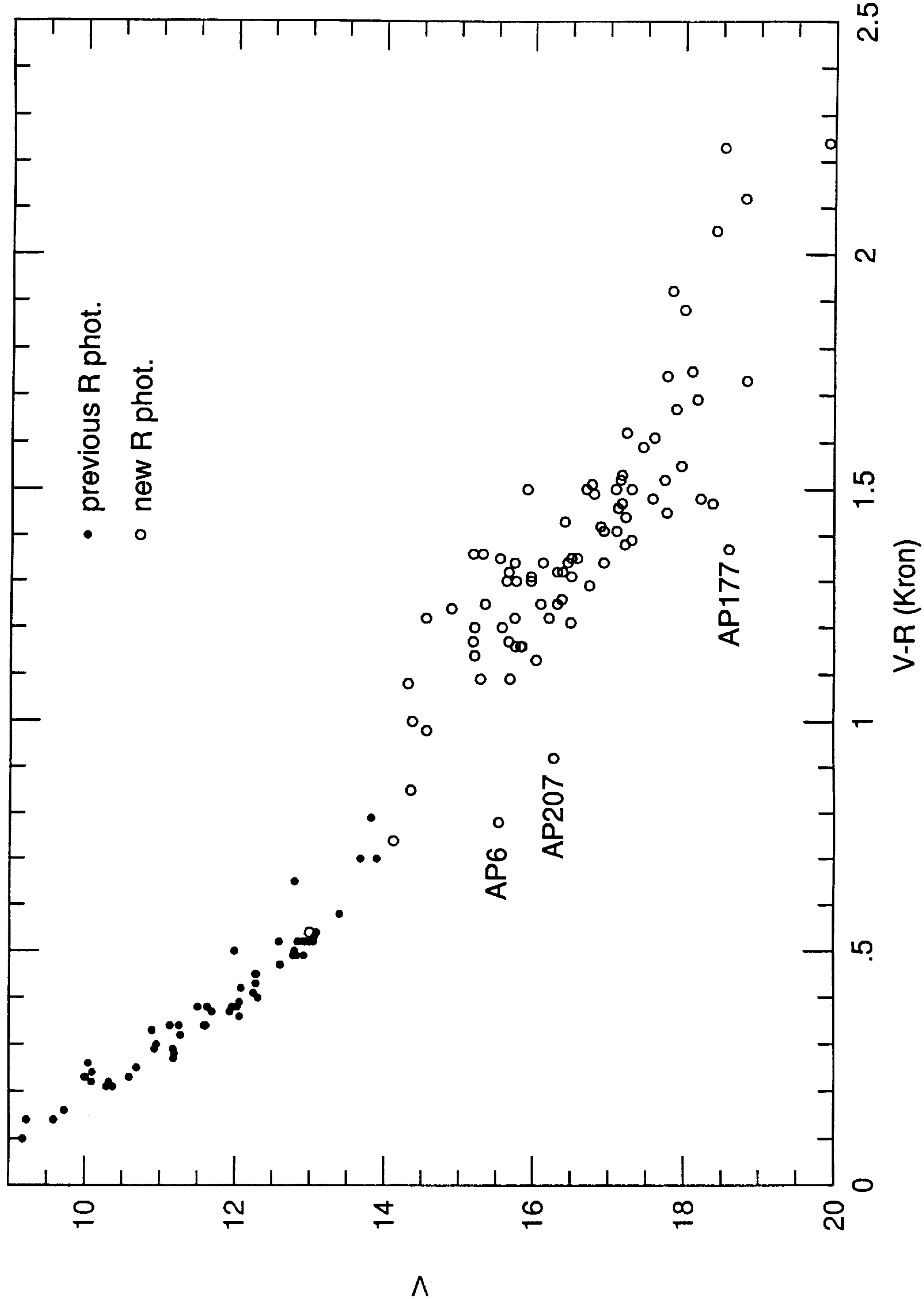

previous R phot.
new R phot.
AP6
AP207
AP177
V-R (Kron)
V
0
.5
1
1.5
2
2.5
10
12
14
16
18
20

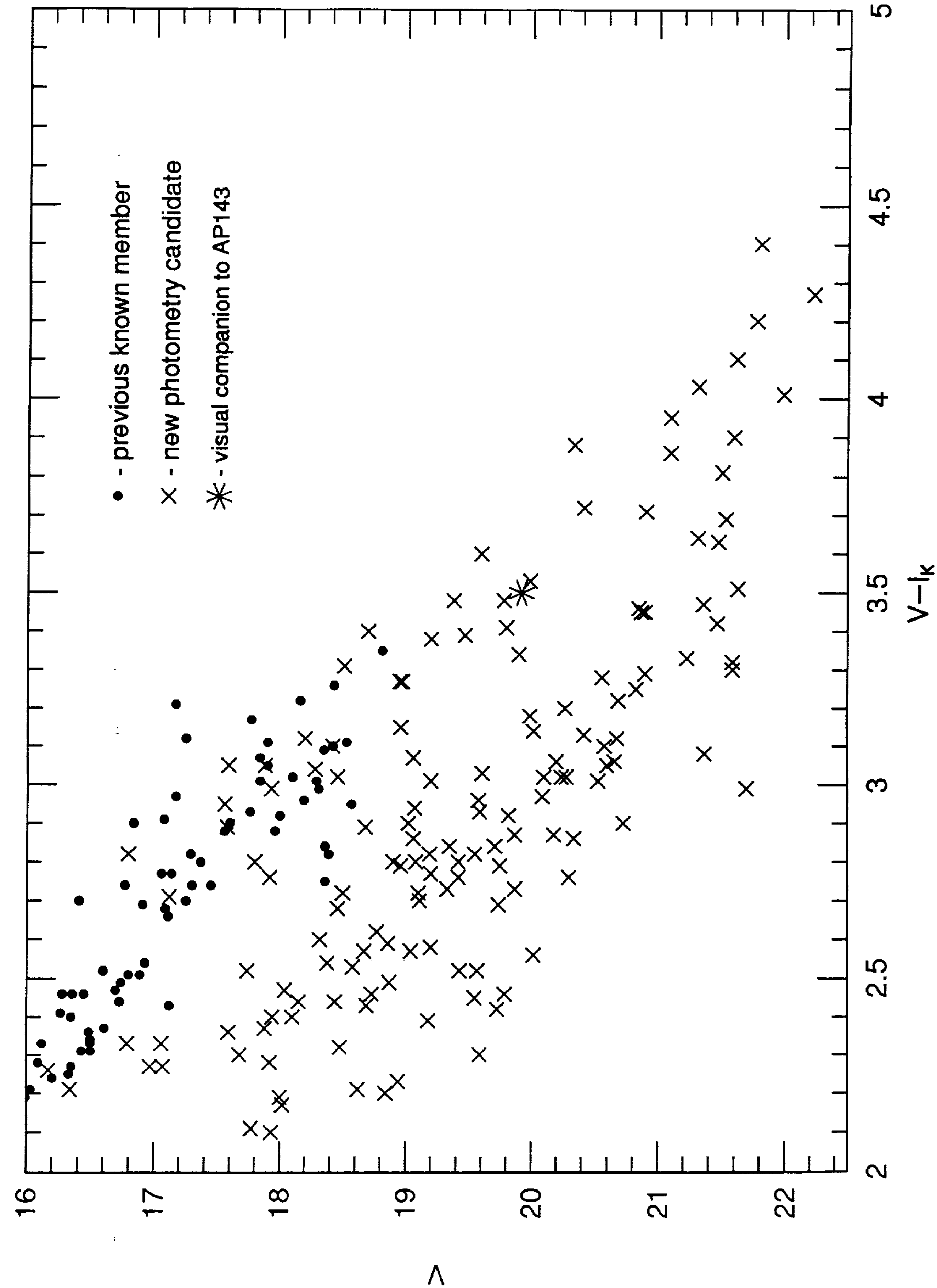
• - previous known member
× - new photometry candidate
✳ - visual companion to AP143
V
V–I_K
16
17
18
19
20
21
22
2
2.5
3
3.5
4
4.5
5

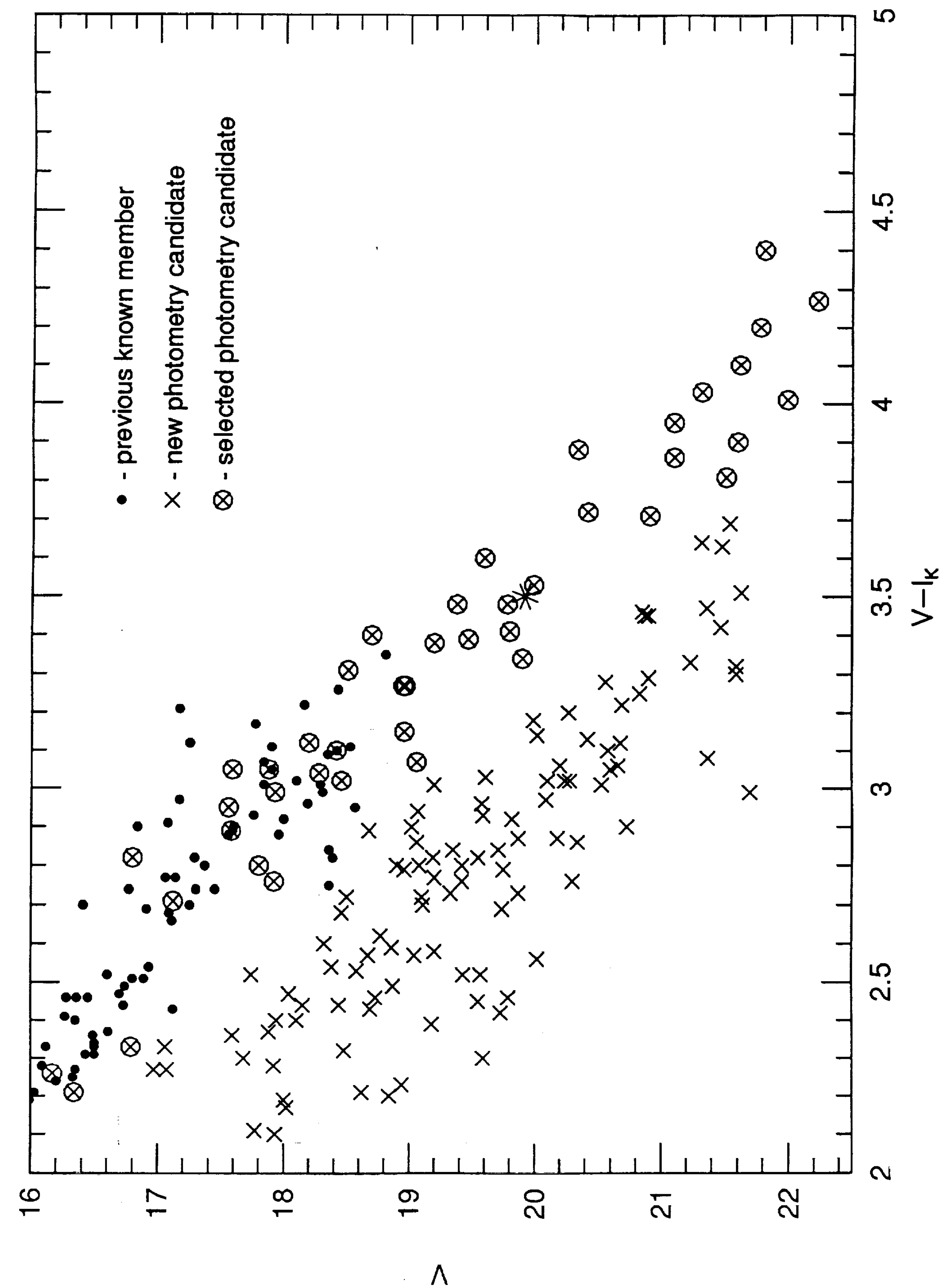
• - previous known member
× - new photometry candidate
⊗ - selected photometry candidate
V−I_K
V
16
17
18
19
20
21
22
2
2.5
3
3.5
4
4.5
5

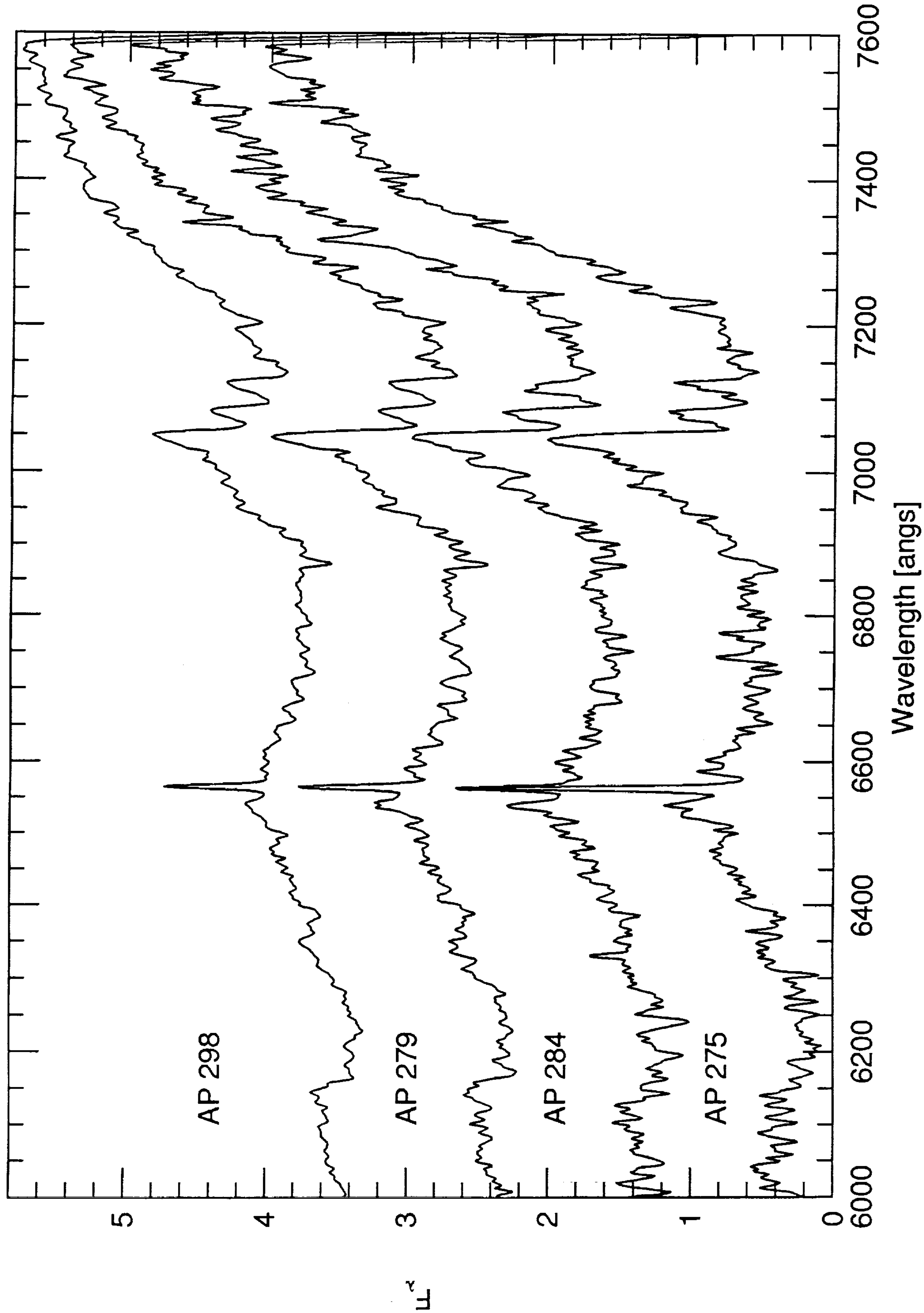
AP 298
AP 279
AP 284
AP 275
Wavelength [angs]
6000
6200
6400
6600
6800
7000
7200
7400
7600
F_λ
0
1
2
3
4
5

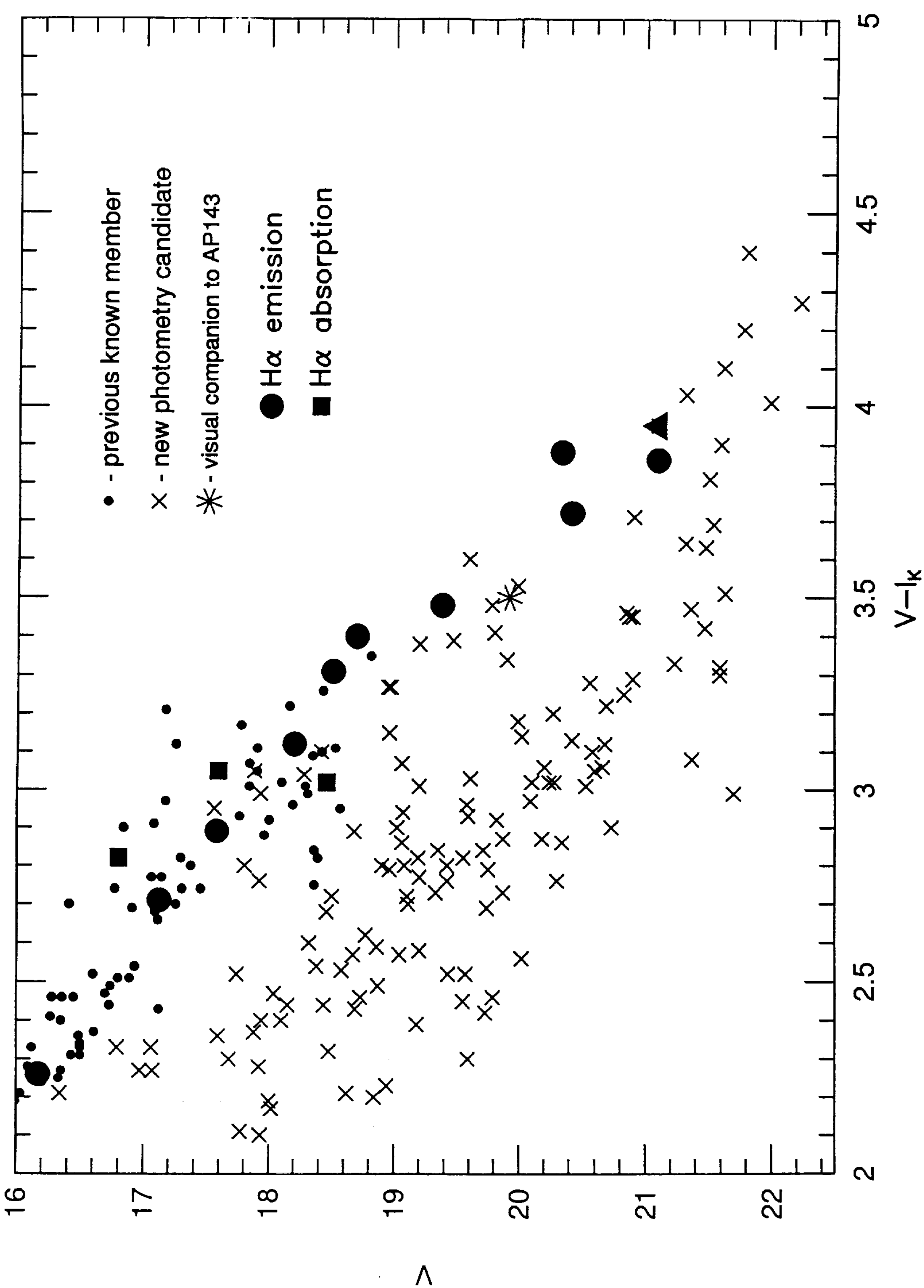
- previous known member
- new photometry candidate
- visual companion to AP143
Hα emission
Hα absorption
V−I_K
V
16
17
18
19
20
21
22
2
2.5
3
3.5
4
4.5
5

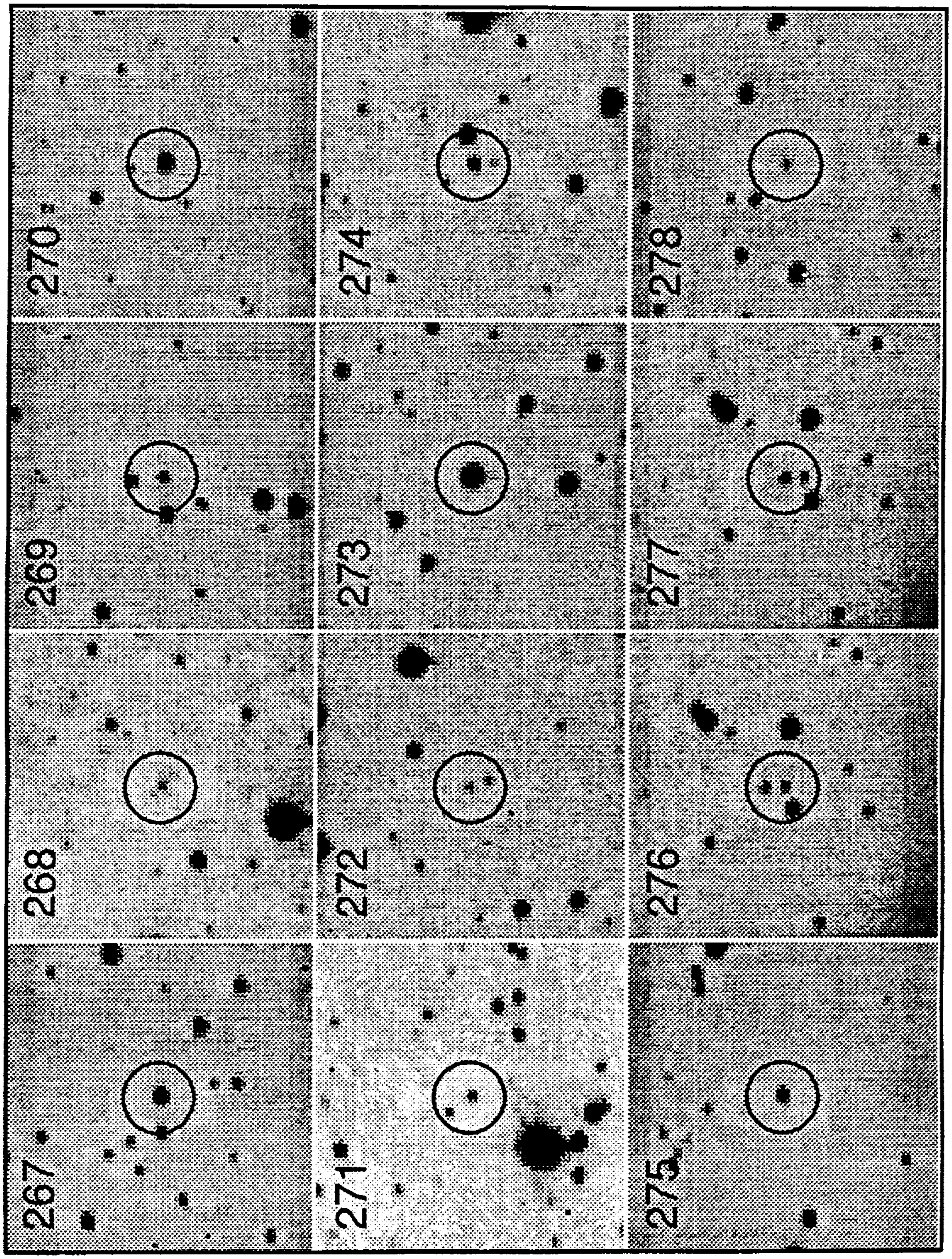
267
268
269
270
271
272
273
274
275
276
277
278

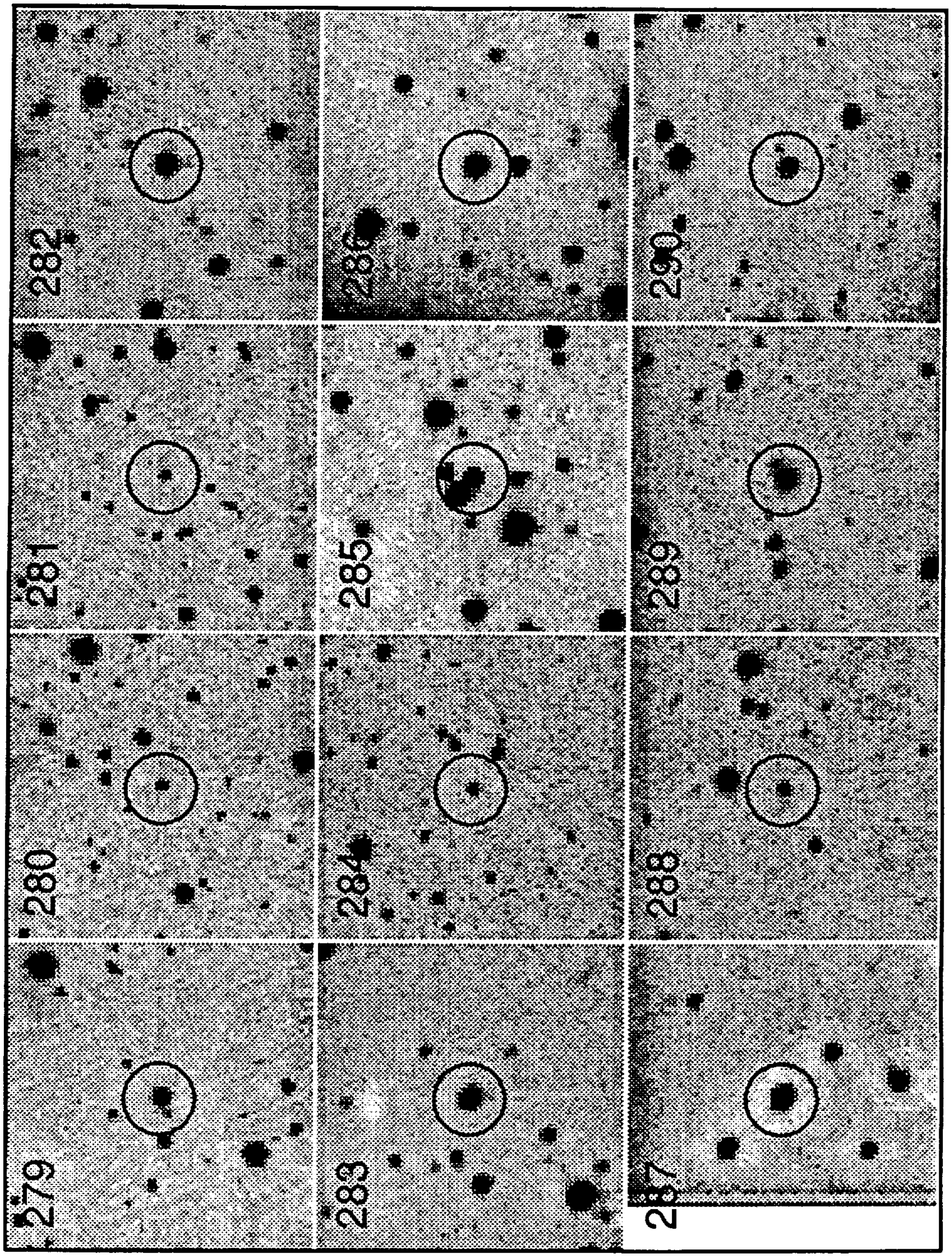
279
280
281
282
283
284
285
286
287
288
289
290

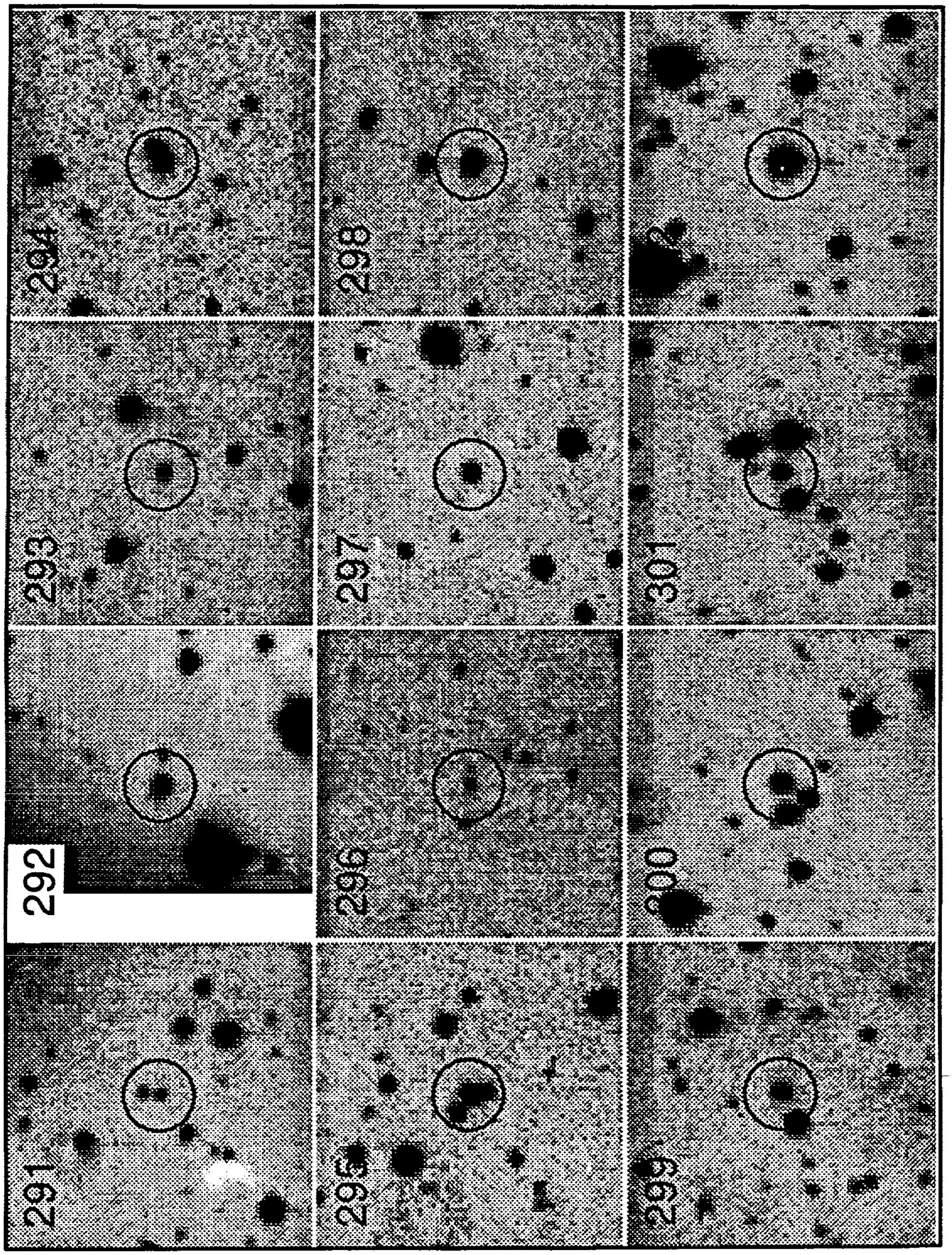
291
292
293
296
297
298
301

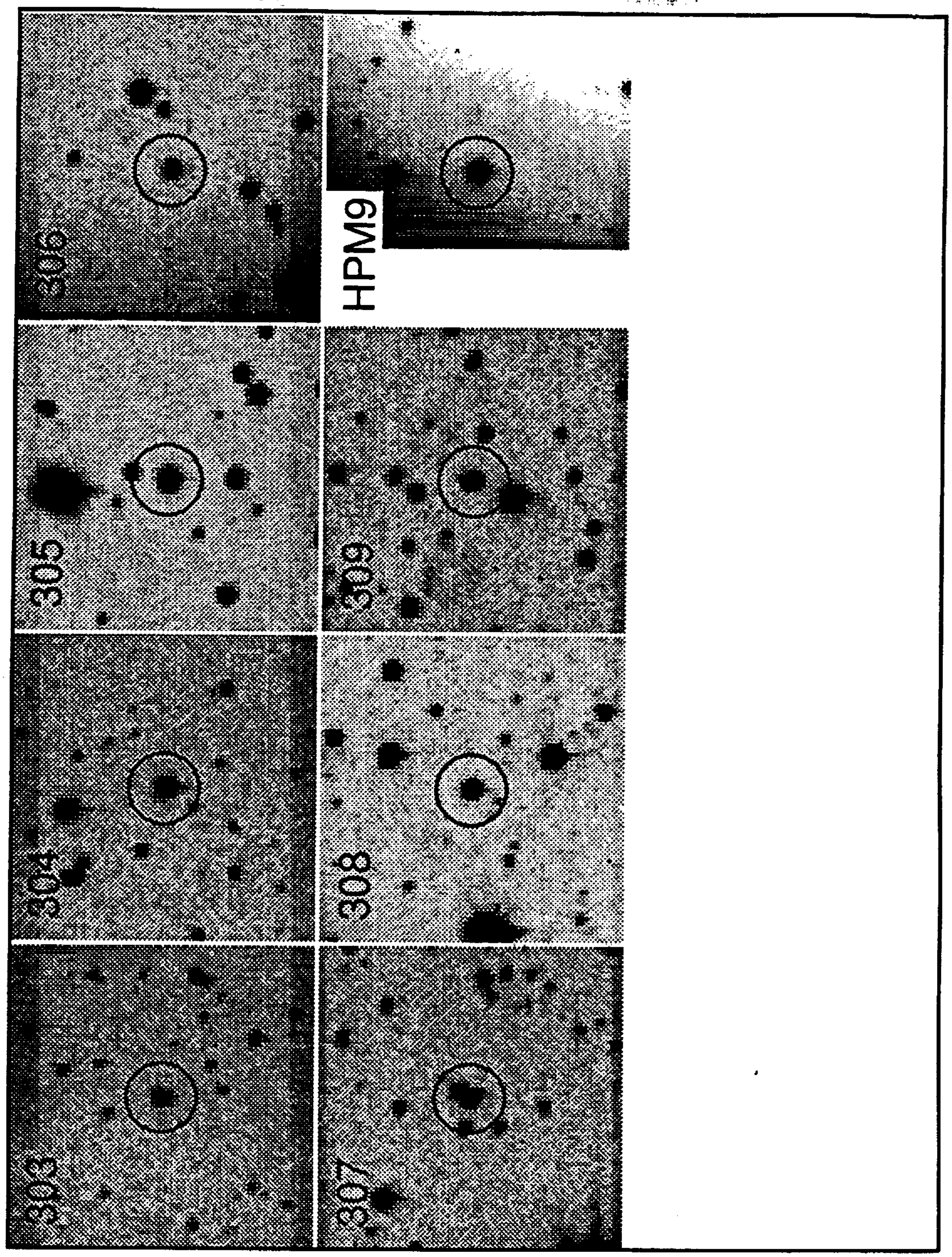
303
304
305
306
307
308
309
HPM9